

Phosphatidylcholine Monolayer Structure at a Liquid–Liquid Interface

Robert A. Walker, Julie A. Gruetzmacher,[†] and Geraldine L. Richmond*

Contribution from the Department of Chemistry, University of Oregon, Eugene, Oregon 97403

Received March 5, 1998

Abstract: Vibrational sum frequency spectroscopy has been used to examine the vibrational structure of phosphatidylcholine monolayers adsorbed to a water–carbon tetrachloride interface. The surfactants employed in this study belong to a family of saturated, symmetric phosphatidylcholines with acyl chain lengths ranging from C₁₂ to C₁₈ in increments of two methylene units. Vibrational spectra provide direct information about the orientation and degree of order among the acyl chains of the adsorbed phosphatidylcholines. Differences among spectra recorded under various polarization conditions show that acyl chains do not exhibit long range order or preferred tilt angle. Rather, acyl chains within a tightly packed monolayer stand up with their methyl C₃ axes aligned perpendicular to the interface. Relative methyl and methylene symmetric stretch band intensities show that order within the monolayer increases with increasing surface coverage. Temperature-dependent studies of monolayer order suggest that a barrier exists to organic solvent penetration of the acyl chain network of a tightly packed, adsorbed monolayer. At a liquid–liquid interface, shorter chain phosphatidylcholine species form monolayers more ordered than those of longer chain species, although the dependence of monolayer order on acyl chain length is small. This trend reverses in monolayers at the air–water interface where longer chain phosphatidylcholines form monolayers dramatically more ordered than those of their shorter chain counterparts. The disparity in behavior between monolayers at the liquid–liquid and air–water interfaces is interpreted as evidence of acyl chain solvation by the organic CCl₄ solvent.

I. Introduction

Given their physiological importance as model systems for biological membranes, phospholipid monolayers have been the subject of intense scientific scrutiny dating back almost three decades.^{1–3} Phospholipids constitute the major component of most cell membranes and consist of a charged headgroup connected to a pair of long acyl chains by means of a three-carbon glycerol backbone (Figure 1). At interfaces, these amphiphilic molecules form Langmuir films which exhibit a host of different phases and morphologies.^{4–6} Understanding the rich thermodynamic behavior found in phospholipid monolayers has helped elucidate the nature of more complex phase behavior which takes place in bilayer systems. Insofar as properties such as permeability, compressibility, and phase-transition temperatures depend on the identity of phospholipid headgroup and acyl chain length, considerable effort has focused on correlating monolayer structure with function.^{7–9} In this paper, we employ interfacially specific, nonlinear optical spectroscopy to examine ordering among the acyl chains in

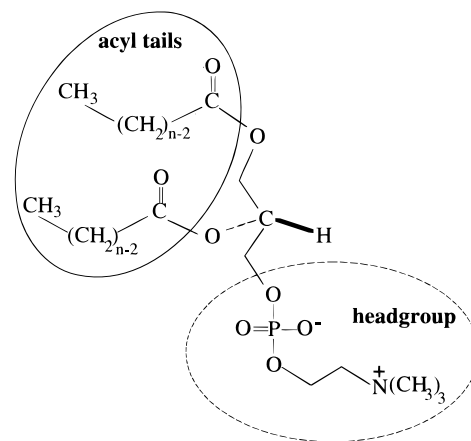


Figure 1. Molecular structure of a saturated, symmetric, diacylphosphatidylcholine. At the experimental pH of 7.0, PC headgroups are zwitterionic. In these studies, acyl chains ranged in length from $n = 12$ (dilauroylphosphatidylcholine, DLPC) to $n = 18$ (distearoylphosphatidylcholine, DSPC) in increments of two methylene units ($n = 14$, dimyristoylphosphatidylcholine, DMPC; $n = 16$, dipalmitoylphosphatidylcholine, DPPC).

[†] Current address: Department of Chemistry, University of Chicago, Chicago, IL 60673.

(1) Jones, M. N.; Chapman, D. *Micelles, Monolayers, and Biomembranes*; Wiley-Liss: New York, 1995.

(2) Cevik, G.; Marsh, D. *Phospholipid Bilayers*; John Wiley and Sons: New York, 1987; Vol. 5.

(3) Phillips, M. C.; Chapman, D. *Biochim. Biophys. Acta* **1968**, *163*, 301–313.

(4) Möhwald, H. *Annu. Rev. Phys. Chem.* **1990**, *41*, 441–476.

(5) McConnell, H. M. *Annu. Rev. Phys. Chem.* **1991**, *42*, 171–195.

(6) Knobler, C. M.; Desai, R. C. *Annu. Rev. Phys. Chem.* **1992**, *43*, 207–236.

(7) MacDonald, R. C.; Simon, S. A. *Proc. Natl. Acad. Sci. U.S.A.* **1987**, *84*, 4089–4093.

(8) Gershfeld, N. L. *Annu. Rev. Phys. Chem.* **1976**, *27*, 349–368.

(9) Blume, A. *Biochim. Biophys. Acta* **1979**, *557*, 32–44.

phosphatidylcholine monolayers adsorbed to a water–carbon tetrachloride interface. Specifically, we show how conformational order depends on surface concentration, temperature, and acyl chain length. By comparing results from monolayers adsorbed to a liquid–liquid interface with those from monolayers spread at an air–water interface, we demonstrate how the organic solvent dramatically affects acyl chain structure.

A wide variety of experimental techniques have characterized the behavior of phospholipid monolayers adsorbed to an air–water interface. Surface pressure measurements constituted the

earliest experiments carried out in this environment.^{3,10} The resulting isotherms demonstrated that monolayers pass through a number of distinct phases as they are compressed from a two-dimensional gas to a tightly packed, two-dimensional solid. More recent experiments have examined the morphology of these phases by means of fluorescence microscopy using labeled phospholipids.^{4–6} Phospholipids form micrometer size domains in the coexistence region between the liquid expanded and liquid condensed states. Theoretical efforts to model this behavior have considered the line tension of different domain shapes⁵ as well as parameters accounting for osmotic pressure between solvated headgroups.¹¹ Additional fluorescence measurements have shown that the acyl chains of tightly packed monolayers form a network that is impervious to gas permeation.¹² Neutron¹³ and X-ray reflection¹⁴ experiments have allowed researchers to infer monolayer thickness and molecular areas as a function of lateral surface pressure. Infrared and Raman studies of acyl CH stretching vibrations indicate that structural changes in the acyl chains accompany phase transitions.^{15,16} Using band positions of modes sensitive to chain conformation, researchers have concluded that in the liquid condensed phase monolayers composed of shorter chain phospholipids contain more gauche defects than monolayers composed of longer chain phospholipids.¹⁷

Compared to our knowledge of phospholipid monolayers at air–water interfaces, information about phospholipid monolayers adsorbed to liquid–liquid interfaces is neither as detailed nor as comprehensive. Making measurements at the boundary between two immiscible liquids poses numerous experimental challenges not encountered in air–water experiments. In addition, given the tremendous diversity of liquid–liquid interfaces, understanding the properties of different monolayers adsorbed to different interfaces becomes a formidable task. Nevertheless, surface tension and fluorescence microscopy studies have shed some light on the varied behavior of phospholipid monolayers in these “buried” environments. Interaction between the organic phase and the phospholipid acyl chains can dramatically affect a particular system’s thermodynamics. For example, surface pressure measurements at a heptane–water interface suggest that monolayers of short chain phospholipids do not pass through any of the discrete phases observed at the air–water interface.^{18–21} Rather, monolayers at this interface smoothly pass from the gaseous to the solid state in one continuous isotherm. Longer chain phospholipids exhibit a single, second-order phase transition from an isotropic, two-dimensional fluid phase to a more tightly packed condensed

phase.¹⁹ This phase transition can be accounted for in a monolayer equation of state if monomers at the interface are allowed to cluster.²² Fluorescence microscopy and X-ray diffraction both indicate that the degree of organic solvent penetration into the acyl region of the monolayer depends on the nature of the phospholipid headgroup and the similarity in solvent and phospholipid chain lengths.^{23,24} Reduced chain–chain interaction due to intercalation of the organic solvent leads to more expanded monolayers at equivalent surface pressures relative to the air–water interface.

Theoretical models predict that the presence of an organic phase affects phospholipid headgroup structure.^{25,26} Due to the hydrophobic effect, the quaternary ammonium of phosphatidylcholines (PC) directs the P–N dipole away from the interfacial plane at an angle of $\sim 15^\circ$ toward the organic phase. In contrast, phosphoethanolamine (PE) headgroups at alkane–water interfaces point into the aqueous phase at a shallower angle due to the amine’s ability to hydrogen bond. Molecular dynamics simulations support this picture. Recent simulation experiments show that lamellar PC bilayers present a much rougher hydrophilic topography to an aqueous solvent than PE bilayers, which assume a more uniform sheetlike structure.^{27–32} Most molecular dynamics studies have examined headgroup and glycerol backbone structure in adjacent bilayers as well as the structure and dynamics of the intervening aqueous solvent.^{27–30,33} Some studies have worked with monolayer systems exclusively, but the emphasis in this work lay in understanding the long range effects of phospholipid headgroups on surrounding water molecules.^{31,34} One set of simulations which specifically investigated acyl chain structure in phospholipid systems was carried out by Chiu et al.³⁵ These experiments demonstrated how acyl chain conformation grows increasingly disordered as a PC bilayer passes from its solid gel state to its more fluid liquid crystalline state.

Given that under many conditions a phospholipid monolayer represents a close approximation to half of a lipid bilayer,³⁶ the experiments described in this paper share some similarities with the molecular dynamics simulations. However, because very few simulations focus on the acyl structure of the lipid bilayer interior, little opportunity exists for direct comparison. We can compare our results with the findings of Chiu et al.,³⁵ while recognizing that our systems consist of PC monolayers which are fully solvated on both the aqueous and organic sides (with

(10) Vilallonga, F. *Biochim. Biophys. Acta* **1968**, *163*, 290–300.
 (11) Feng, S.; Brockman, H. L.; MacDonald, R. C. *Langmuir* **1994**, *10*, 3188–3194.
 (12) Caruso, F.; Grieser, F.; Thistlethwaite, P. J.; Almgren, M.; Wistus, E.; Mukhtar, E. *J. Phys. Chem.* **1993**, *97*, 7364–7370.
 (13) Bayerl, T. M.; Thomas, R. K.; Penfold, J.; Rennie, A.; Sackman, E. *Biophys. J.* **1990**, *57*, 1095–1098.
 (14) Brezesinski, G.; Thoma, M.; Struth, B.; Möhwald, H. *J. Phys. Chem.* **1996**, *100*, 3126–3130.
 (15) Gericke, A.; Moore, D. J.; Erukulla, R. K.; Bittman, R.; Mendelsohn, R. *J. Mol. Struct.* **1996**, *379*, 227–239.
 (16) Hunt, R. D.; Mitchell, M. L.; Dluhy, R. A. *J. Mol. Struct.* **1989**, *214*, 93–109.
 (17) Dluhy, R. A.; Wright, N. A.; Griffiths, P. R. *Appl. Spectrosc.* **1988**, *42*, 138–141.
 (18) Mingins, J.; Stigter, D.; Dill, K. A. *Biophys. J.* **1992**, *61*, 1603–1615.
 (19) Mingins, J.; Taylor, J. A. G.; Pethica, B. A.; Jackson, C. M.; Yue, B. Y. *J. Chem. Soc., Faraday Trans.* **1982**, *78*, 323–339.
 (20) Taylor, J. A. G.; Mingins, J.; Pethica, B. A. *J. Chem. Soc., Faraday Trans. 1* **1976**, *12*, 2694–2702.
 (21) Yue, B. Y.; Jackson, C. M.; Taylor, J. A. G.; Mingins, J.; Pethica, B. A. *J. Chem. Soc., Faraday Trans. 1* **1976**, *72*, 2685–2693.

(22) Ruckenstein, E.; Li, B. *Langmuir* **1996**, *12*, 2308–2315.
 (23) Thoma, M.; Möhwald, H. *J. Colloid Interface Sci.* **1994**, *162*, 340–349.
 (24) Thoma, M.; Möhwald, H. *Colloids Surf., A* **1995**, *95*, 193–200.
 (25) Stigter, D.; Mingins, J.; Dill, K. A. *Biophys. J.* **1992**, *61*, 1616–1629.
 (26) Dill, K. A.; Stigter, D. *Biochemistry* **1988**, *27*, 3446–3453.
 (27) Pink, D. A.; Belaya, M.; Levadny, V.; Quinn, B. *Langmuir* **1997**, *13*, 1701–1711.
 (28) Damodaran, K. V.; Merz, K. M. *Biophys. J.* **1994**, *66*, 1076–1087.
 (29) Essmann, U.; Perera, L.; Berkowitz, M. L. *Langmuir* **1995**, *11*, 4519–4531.
 (30) Perera, L.; Essmann, U.; Berkowitz, M. L. *Langmuir* **1996**, *12*, 2625–2629.
 (31) Alper, H. E.; Bassolino, D.; Stouch, T. R. *J. Chem. Phys.* **1993**, *98*, 9798–9807.
 (32) Raghavan, K.; Reddy, M. R.; Berkowitz, M. L. *Langmuir* **1992**, *8*, 233–240.
 (33) Tieleman, D. P.; Berendsen, H. J. C. *J. Chem. Phys.* **1996**, *105*, 4871–4880.
 (34) Alper, H. E.; Bassolino-Klimas, D.; Stouch, T. R. *J. Chem. Phys.* **1993**, *99*, 5547–5559.
 (35) Chiu, S. W.; Clark, M.; Balaji, V.; Subramaniam, S.; Scott, H. L.; Jakobsson, E. *Biophys. J.* **1995**, *69*, 1230–1245.
 (36) McIntosh, T. J.; Simon, S. A.; MacDonald, R. C. *Biochim. Biophys. Acta* **1980**, *597*, 445–463.

water and CCl_4 , respectively), while the bilayer interior studied in simulations contained no explicit organic solvent.

In the experiments described below, the phospholipids used belong to a series of saturated, symmetric, diacyl phosphatidylcholines (Figure 1) with chains ranging in length from C_{12} (dilauroyl-*sn*-phosphatidylcholine, DLPC) to C_{18} (distearoyl-*sn*-phosphatidylcholine, DSPC) in increments of two methylene units (C_{14} = dimyristoyl-*sn*-phosphatidylcholine, DMPC; C_{16} = dipalmitoyl-*sn*-phosphatidylcholine, DPPC). To form monolayers at an aqueous-carbon tetrachloride interface from a solution of phosphatidylcholine vesicles, we rely upon decomposition of vesicles to deposit PC monomers at the boundary between the two immiscible solvents.³⁷ Interfacial PC concentrations are controlled by fixing the bulk aqueous phase PC concentration and the system's temperature. Surface pressure measurements monitor the extent of monolayer formation and vibrational sum frequency spectroscopy, an interfacially specific, nonlinear optical technique, elucidates the molecular structure of the acyl chains which make up the monolayer. We emphasize that this method of preparing monolayers involves a slow, gradual approach to the final monolayer composition, which allows the monolayer to remain equilibrated as the surface concentration increases. Recent experiments have shown how repeated multiple injection techniques which physically perturb the interface can lead to a metastable two-dimensional crystallization of long chain phosphatidylcholine monolayers adsorbed to the aqueous- CCl_4 interface.³⁸

This paper is organized as follows: we begin by describing sample preparation, monolayer characterization, the origin of the vibrational sum frequency (VSF) signal, and the relevant alkyl chain spectroscopy. Next, a series of spectra show how different choices of polarization disclose different aspects of acyl chain orientation within monolayers. Tightly packed phosphatidylcholine monolayers³⁹ adsorbed to the aqueous- CCl_4 interface adopt a rotationally invariant distribution about the interface normal, leaving the C_3 axes of the acyl methyl groups perpendicular to the interface. Spectra are shown for the case of DLPC although this behavior is general for all PCs studied. In subsequent sections we examine how chain structure depends on both DLPC surface coverage and interfacial temperature. Not surprisingly, chains become more ordered with increasing surface concentration. Acyl chain structure appears insensitive to changes in temperature below ambient conditions ($T < 20$ °C). Above 20 °C, however, acyl chain structure becomes more disordered with increasing temperature. We attribute this phenomenon to an increased agitation of the acyl chains and thermally induced solvent permeation of the CCl_4 into the acyl chain network. Finally, we study order within a tightly packed monolayer as a function of chain length for monolayers at the water-carbon tetrachloride interface and contrast these findings with those from PC monolayers with similar surface concentrations at an air-water interface. At the liquid-liquid interface, the shorter chain PCs form more ordered monolayers than the longer chain PCs although the effect of chain length is slight. This trend reverses and amplifies at the

(37) Walker, R. A.; Conboy, J. C.; Richmond, G. L. *Langmuir* **1997**, *13*, 3070-3073.

(38) Smiley, B. L.; Richmond, G. L. *J. Phys. Chem. B*, submitted for publication.

(39) Throughout this paper, the term "tightly packed" refers to monolayers having concentrations of 1.8×10^{14} molecules/cm² or, equivalently, 55 Å²/molecule. Without external means for monolayer compression, we rely on the equilibrium existing between aqueous-phase PC vesicles and adsorbed PC monomers to create monolayers having different surface concentrations. The most tightly packed monolayer formed under these circumstances has a molecular area of 55 Å²/molecule regardless of chain length.

air-water interface where order among the acyl chains increases dramatically with increasing chain length. These results suggest that at the liquid-liquid interface CCl_4 intercalates into the acyl monolayer network, screening the chains from attractive, interchain van der Waals forces.

II. Experimental Section

A. Sample Preparation. The four different phosphatidylcholines used in these studies were purchased as lyophilized powders from Avanti Polar Lipids (>99.9% pure) and used as received. The aqueous phase consisted of either H_2O (Millipore, 18 MΩ) or D_2O (Aldrich, 99.9%) that had been saturated with CCl_4 and buffered with a sodium phosphate solution to a pH of 7.0 (10 mM in phosphate ion). Carbon tetrachloride (Aldrich, reagent grade or Baker, reagent grade) had its purity confirmed by FTIR and ¹H NMR. Interfacial tension measurements of the neat water-carbon tetrachloride interface produced results in agreement with literature values,⁴⁰ indicating an absence of any surface active contaminants in the two solvents.

In aqueous solution, phosphatidylcholines spontaneously aggregate to form bilayer sheets. Upon sonication, these sheets rearrange to form uni- or multilamellar bilayer vesicles. The thermodynamic phase of these bilayer vesicles depends on the temperature of the solution; at low temperatures the bilayer interiors are frozen in a gel phase, while at higher temperatures the chains melt and assume a more fluid, disordered liquid crystalline phase. Stock solutions of PC vesicles were prepared by suspending a measured amount of phosphatidylcholine in 10 mL of either buffered H_2O or D_2O and then sonicating the solution at a temperature above the appropriate phase-transition temperature.⁴¹ This procedure created a solution of vesicles ranging in diameter from 60 to 150 nm as determined from dynamic light scattering measurements. Typical concentrations of these stock solutions ranged from 0.5 to 2.0 mM. Phosphatidylcholine concentrations reported in the experiments discussed below resulted from gentle, small volume additions of a stock solution to an aqueous phase of PC-free buffer solution.

Phosphatidylcholine stock solutions used immediately after sonication showed a greater surface activity than stock solutions which had aged even just several hours. After preparing a phosphatidylcholine stock solution, we allowed a minimum of 10-12 h to elapse before making a small volume addition and beginning an experiment. Further waiting led to no additional change in PC surface activity. This observation agrees with the findings of Qiu and MacDonald, who reported the existence of metastable, highly surface-active species in freshly sonicated phospholipid solutions.⁴² These species are attributed to "open" shell vesicles which, over time, rearrange or aggregate to form more stable, closed shell structures. Stock solutions were replaced every 5 days.

B. Spectroscopic Technique. Vibrational spectra of the phosphatidylcholine monolayers adsorbed to the H_2O - CCl_4 interface were acquired using vibrational sum frequency spectroscopy (VSFS) in a total internal reflection (TIR) geometry.⁴³ Spectra of phosphatidylcholine monolayers at the air-water interface were collected with an external reflection geometry. In the TIR geometry, the visible and infrared beams passed through the high index medium (CCl_4) and approached the interface at their respective critical angles. The sum frequency (SF) signal was collected in reflection. When probing the air-water interface, both incident beams approached the surface from the air and again the signal was collected in reflection.

Two different laser systems were employed to collect spectra presented in this paper. Both have been described previously.^{43,44} To generate the visible and infrared frequencies used in the H_2O - CCl_4

(40) Adamson, A. W. *Physical Chemistry of Surfaces*, 4th ed.; John Wiley and Sons: New York, 1982.

(41) Gregoriadis, G. *Liposome Technology*; CRC Press: Boca Raton, 1984; Vol. 1.

(42) Qiu, R.; MacDonald, R. C. *Biochim. Biophys. Acta* **1994**, *1191*, 343-353.

(43) Conboy, J. C.; Messmer, M. C.; Richmond, G. L. *J. Phys. Chem.* **1996**, *100*, 7617-7622.

(44) Gragson, D. E.; Alavi, D. S.; Richmond, G. L. *Opt. Lett.* **1995**, *20*, 1991-1993.

studies, the output of an extended cavity Nd:YAG laser (Quanta Ray GCR11, 13 ns pulse width) was split into two parts. One part of the 1064 nm output was frequency doubled in a KDP crystal to provide 5–10 mJ of fixed-frequency 532 nm radiation. The second part of the 1064 nm output pumped a home-built, angle-tuned LiNiO₃ optical parametric oscillator to provide 1–3 mJ of infrared radiation in the 3 μm region with a bandwidth of 6 cm^{-1} . At the interface, the 532 nm beam had a diameter of ~ 3 mm while a CaF₂ lens focused the infrared down to a spot diameter of ~ 150 μm . The cell used in these studies consisted of a 5-cm long quartz cylinder (10-cm diameter) with Teflon caps sealing both ends. Caps contained ports through which additions of PC stock solution could be made to the aqueous phase. An interface was created by first adding ~ 150 mL of CCl₄ to the cell followed by 40 mL of PC-free, aqueous buffer which rested upon the organic phase. VSF spectra of these neat interfaces showed them to be free of surface-active organic contaminants.

Spectra at the air–water interface were acquired using a regeneratively amplified Ti:sapphire laser system which produced 800 μJ of 800-nm light at a repetition rate of 1 kHz and with a pulse width of 2 ps. Part of the 800-nm output pumped a white light/KTP optical parametric amplifier assembly which generated tunable infrared radiation (2.8–3.7 μm , ~ 5 μJ , 16 cm^{-1} spectral bandwidth). The remaining 800-nm output provided the fixed-frequency component in the VSF experiments. We prepared phosphatidylcholine monolayers at the air–water interface by means of a hexane–ethanol spreading solvent (4:1 by volume) in a shallow 6-cm diameter crystallizing dish. Spectra of the neat surface showed an absence of surface-active contaminants, and spectra of the surface following addition of phosphatidylcholine-free spreading solvent indicated that the spreading solvent evaporated within 30 s after deposition, leaving behind a clean interface.

C. Interfacial Tension. Interfacial tension measurements at the water–carbon tetrachloride interface were carried out with a Wilhelmy plate microbalance assembly and a 6-cm diameter glass crystallizing dish. An experiment required deposition of a 20-mL aliquot of CCl₄ into the dish followed by a gentle 20-mL addition of PC-free aqueous solution. With the interface established, a platinum plate was lowered so that its top edge lay submerged beneath the water and its bottom edge extended ~ 2 mm below the nominal water–CCl₄ interface. All measurements began by monitoring the tension of the neat interface. Once interfacial stability and purity had been confirmed, a small volume (0.05–1 mL) of PC stock solution was added to the aqueous phase to raise the bulk aqueous PC concentration to the desired value. (Additions of 1 mL PC-free buffer to the 20-mL aqueous phase were found to change the surface tension by < 1 mN/m). The surface tension (γ) decreased following addition of PC stock solution, slowly approaching an equilibrium value. Terminal $\gamma(t)$ readings were recorded when the rate of change of $\gamma(t)$ fell to less than 2% of $\gamma_0 - \gamma(t)$ per hour. Values of terminal $\gamma(t)$ were converted to surface pressures ($\Pi = \gamma_0 - \gamma(t)$) and plotted versus bulk phosphatidylcholine concentration in order to map out adsorption isotherms and measure the extent of monolayer formation. Terminal surface pressures of tightly packed monolayers adsorbed to the water–carbon tetrachloride interface agreed reasonably well with reported results of phosphatidylcholine monolayers adsorbed to alternative aqueous–organic interfaces.^{18,19,45}

III. Spectroscopic Background

A. Vibrational Sum Frequency Spectroscopy. One constraint limiting understanding of molecular structure at condensed phase interfaces has been the dearth of experimental techniques that not only access these interfaces but also discriminate responses of these interfaces from responses of the respective bulk materials. However, due to recent improvements in the generation of tunable, coherent infrared sources, VSFs has developed into a powerful technique for probing molecular structure at solid–liquid,⁴⁶ solid–air,⁴⁷ liquid–air,⁴⁸ and liquid–liquid interfaces.⁴⁹ This method has proven remarkably sensitive to submonolayer coverage and subtle changes in molecular

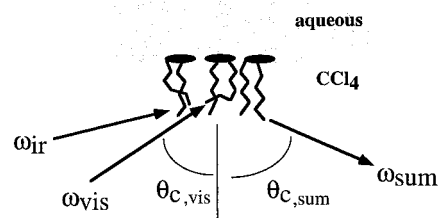


Figure 2. Diagram of a vibrational sum frequency experiment in a total internal reflection geometry with a phospholipid monolayer adsorbed to the water–CCl₄ interface. All beams pass through the high index CCl₄ medium with the visible (ω_{vis}) and sum frequency (ω_{sum}) fields propagating at their critical angles, $\theta_{\text{c,vis}}$ and $\theta_{\text{c,sum}}$, respectively. The infrared beam (ω_{IR}) is tunable from 2800 to 3000 cm^{-1} .

conformation at interfaces. The technique of VSFs involves two coherent optical fields, typically one fixed-frequency visible and one tunable infrared, converging spatially and temporally on the interface (Figure 2). When the infrared radiation is resonant with an allowed vibrational transition of a molecule at the interface, the two fields interact through the resonant component of the second-order nonlinear susceptibility ($\chi^{(2)}$) to create a third optical field equal in energy to the sum of the visible and infrared energies.

A molecule under the influence of oscillating electric fields experiences a time-dependent polarization which can be expressed as an expansion in its polarizability,

$$P(\omega_1, \omega_2, t) = P^{(0)} + P^{(1)} + P^{(2)} + \dots \quad (1)$$

The second-order term in the polarization expression is responsible for sum frequency generation and can be expressed in terms of incident electric fields and the second-order susceptibility $\chi^{(2)}$,

$$P^{(2)} = \chi^{(2)} : E_1(t)E_2(t) \quad (2)$$

Here, E_1 and E_2 are the visible (ω_{vis}) and infrared (ω_{IR}) fields, and $\chi^{(2)}$ is the second-order susceptibility. Because $\chi^{(2)}$ is a third-rank tensor, it must change sign with respect to inversion (e.g., $\chi_{ijk}^{(2)} = -\chi_{-i-j-k}^{(2)}$, where ijk refer to coordinates in the laboratory frame of reference). This situation requires that second-order optical processes be forbidden in isotropic media (which are invariant to inversion symmetry) but allowed at surfaces and interfaces between materials where bulk inversion symmetry is necessarily broken.⁵⁰

Although the second-order susceptibility tensor contains twenty-seven different elements, many of these elements reduce to zero under the constraints of a system's symmetry. Applying $C_{\infty v}$ symmetry to an interface leads to only four surviving, nonzero elements, $\chi_{zzz}^{(2)}$, $\chi_{zii}^{(2)}$, $\chi_{izi}^{(2)}$, $\chi_{iiz}^{(2)}$, where $i = x$ or y . When ω_{vis} does not lie near electronic resonances, Kleinmann symmetry renders $\chi_{izi}^{(2)}$ and $\chi_{zii}^{(2)}$ equivalent.⁵¹ Selecting different polarizations of the incident infrared and visible and reflected sum frequency fields samples different subsets of these $\chi^{(2)}$ elements:

(46) Bain, C. D. *J. Chem. Soc., Faraday Trans.* **1995**, *91*, 1281–1296.

(47) Shen, Y. R. *Nature* **1989**, *337*, 519–525.

(48) Eisenthal, K. B. *Chem. Rev.* **1996**, *96*, 1343–1360.

(49) Richmond, G. L. *Anal. Chem.* **1997**, *69*, 536A–543A.

(50) Shen, Y. R. *The Principles of Nonlinear Optics*; John Wiley and Sons: New York, 1984.

(51) Dick, B.; Gierulski, A.; Marowsky, G.; Reider, G. A. *Appl. Phys. B* **1985**, *38*, 107–116.

(45) Li, J.; Fainerman, V. B.; Miller, R. *Langmuir* **1996**, *12*, 5138–5142.

$$I_{ppp} \propto |\tilde{f}_{zffz}\chi_{zzz}^{(2)} + \tilde{f}_{zffz}\chi_{zii}^{(2)} + \tilde{f}_{zffz}\chi_{izi}^{(2)} + \tilde{f}_{zffz}\chi_{iiz}^{(2)}|^2 \quad (3a)$$

$$I_{ssp} \propto |\tilde{f}_{zffz}\chi_{iiz}^{(2)}|^2 \quad (3b)$$

$$I_{sps} \propto |\tilde{f}_{zffz}\chi_{izi}^{(2)}|^2 \quad (3c)$$

Here, the subscripts on the sum frequency intensity refer to the polarization of the sum frequency, visible, and infrared fields in order of descending frequency. The linear and nonlinear Fresnel factors are represented by f_i and \tilde{f}_i , respectively. Equation 3a shows that the choice of $p_{\text{sumPvisPIR}}$ (ppp) polarizations samples all nonzero $\chi^{(2)}$ elements. However, selecting the $s_{\text{sumSvisPIR}}$ condition (ssp) probes only those vibrations having a component of their infrared transition moments aligned normal to the interface. Spectra taken under $s_{\text{sumPvisSIR}}$ (sps) conditions sample vibrations with infrared transition dipoles aligned parallel to the interface.

The nonzero elements of the $\chi^{(2)}$ tensor can be further broken down into nonresonant and resonant pieces:⁴⁶

$$\chi_{ijk}^{(2)} = \chi_{ijk, nr}^{(2)} + \sum_v \chi_{ijk, v}^{(2)} \quad (4)$$

For systems with low polarizabilities, the nonresonant term, $\chi_{ijk, nr}^{(2)}$, is very small and the resonant term represents the dominant contribution to the observed VSF intensity. The resonant piece of $\chi^{(2)}$ is summed over all vibrational resonances contributing to the second-order susceptibility. $\chi^{(2)}$ can be directly related to the number of molecules sampled and the molecular hyperpolarizability, β , by the expression

$$\chi_{ijk, v}^{(2)} = \frac{n}{\epsilon_0} \langle \beta_v \rangle \quad (5)$$

where the brackets on β indicate an orientationally averaged ensemble. The ijk coordinates of the laboratory fixed frame are related to the molecular coordinates of β by means of the direction cosines.⁵² Under the electric dipole approximation, β is directly proportional to a product of the infrared and Raman transition matrix elements, A_v and $M_{v, g}$, respectively,

$$\beta_v = \frac{A_v M_{v, g}}{\omega_{\text{IR}} - \omega_0 - i\Gamma} \quad (6)$$

Here ω_{IR} represents the tunable infrared field, ω_0 is the center frequency of the vibrational transition, and Γ corresponds to the vibrational transition width. Two elements are worth noting about this expression. First, vibrational transitions in centrosymmetric molecules are sum frequency forbidden (by mutual exclusion). Second, β shows very peaked behavior in the vicinity of an allowed vibrational transition due to the difference in the denominator. This resonance condition of β is responsible for the intensity observed in VSF spectra.

B. Acyl Chain Spectroscopy. Tunable infrared radiation in the 3- μm region renders our VSFS experiments particularly sensitive to CH stretching motion. The vibrational spectroscopy of hydrocarbon chains has been thoroughly examined in the literature,^{53–55} although assigning features between 2800 and

3050 cm^{-1} can sometimes prove challenging. For long alkyl chains, spectral complexity arises due to the number of contributing oscillators. Two vibrational motions, the symmetric stretches of the methylene and methyl groups, will play an important role in the analysis presented below. When an alkyl chain assumes an all-trans conformation, the methylene symmetric stretch (d^+) consists of concerted motion of all CH_2 units, assuming C_{2h} symmetry about the center of each carbon-carbon bond. The infrared-active methylene symmetric stretch ($d^+(\Pi)$) is 180° out of phase with the Raman-active methylene symmetric stretch ($d^+(0)$).⁵³ This phase relation leads to a vanishing numerator in eq 6 rendering the methylene symmetric stretch sum frequency *inactive* for an all-trans alkyl chain. The methyl symmetric stretch (r^+) is always sum frequency allowed. Introducing gauche defects or simply allowing for torsional distortion along the carbon backbone lifts the phase constraint placed upon d^+ and the vibrational mode becomes sum frequency active. Consequently, *the intensity ratio of r^+/d^+ in a given spectrum provides a sensitive measure of conformational order among the acyl chains in the monolayer.* A large r^+/d^+ ratio indicates a high degree of conformational order within the monolayer, while a small r^+/d^+ ratio implies a disordered monolayer.

In an absolute sense, this r^+/d^+ ratio may appear to overestimate the degree of acyl chain disorder in the monolayer, since r^+ only measures disorder at the end of the chain while d^+ measures average disorder from many more potentially contributing CH_2 groups. However, as an indicator of how the relative disorder within a monolayer depends on chain length, the r^+/d^+ ratio accurately describes trends under a variety of experimental circumstances.^{56–58}

Quantitative interpretation of r^+/d^+ in terms of absolute acyl chain structure is further complicated by questions about the effects which solvents may have on the inter- and intramolecular potentials governing chain conformation. These issues have direct consequences for the intensity of the d^+ band observed in the VSF spectra. In the absence of an organic solvent, the hydrocarbon chains experience attractive van der Waals interactions which strengthen as the chains become longer. This effect manifests itself in monolayers growing more ordered as chain length increases.⁵⁹ Solvating the chains with small nonpolar solvents can reduce or eliminate these intermolecular forces, meaning that increasing chain length simply increases the opportunity for conformational disorder. Spectra of monolayers formed from ionic, soluble surfactants at the water- CCl_4 interface suggest that the organic solvent does, indeed, influence acyl chain structure.⁵⁶ If the CCl_4 solvates the PC acyl chains, we would expect monolayers to be more disordered at the water- CCl_4 interface than at an air-water interface.

Evidence for changes in the intramolecular torsional potentials of hydrocarbon chains comes from neutron diffraction studies of neat alkane liquids.⁶⁰ The nominal “trans” conformation for alkyl chains (C_4 – C_{20}) in neat liquids includes average dihedral angles of 170° rather than the 180° found in a simple 3-fold potential with minima for the trans and two equivalent gauche conformations. In monolayers, such torsional distortion would lift the symmetry constraint which forbids the d^+ band from

(56) Conboy, J. C.; Messmer, M. C.; Richmond, G. L. *J. Phys. Chem. B*, submitted for publication.

(57) Miranda, P. B.; Pflumio, V.; Saijo, H.; Shen, Y. R. *Chemical Physics Lett.* **1997**, *264*, 387–392.

(58) Bell, G. R.; Bain, C. D.; Ward, R. N. *J. Chem. Soc., Faraday Trans.* **1996**, *92*, 515–523.

(59) Gericke, A.; Hühnerfuss, H. *J. Phys. Chem.* **1993**, *97*, 12899–12908.

(60) Habenschuss, A.; Narten, A. H. *J. Chem. Phys.* **1990**, *92*, 5692–5699.

(52) Hirose, C.; Akamatsu, N.; Domen, K. *Appl. Spectrosc.* **1992**, *46*, 1051–1072.

(53) Snyder, R. G.; Scherer, J. R. *J. Chem. Phys.* **1979**, *71*, 3221–3228.

(54) Snyder, R. G.; Strauss, H. L.; Elliger, C. A. *J. Phys. Chem.* **1982**, *86*, 5145–5150.

(55) MacPhail, R. A.; Strauss, H. L.; Snyder, R. G.; Elliger, C. A. *J. Phys. Chem.* **1984**, *88*, 334–341.

Table 1. Spectral Assignments

band position (cm ⁻¹)	assignment	description	polarization comb.	ref
2850	d^+	CH ₂ symmetric stretch	ssp, sps (weak), ppp	53
2874	r^+	CH ₃ symmetric stretch	ssp, ppp	55
2890–2910		CH ₂ Fermi resonance	ssp, sps, ppp	54
2935	d^-	CH ₂ antisymmetric stretch	ssp, ppp	48,54
~2935		CH ₃ Fermi resonance	ssp, ppp	45,55
2960	r^-	CH ₃ antisymmetric stretch	sps, ppp	55
2985		symmetric choline CH ₃ stretch	sps, ppp	57

appearing in VSF spectra of nominally all-trans acyl chains. (Here, “all-trans” refers to dihedral angles of 180°.) If the organic CCl₄ solvates the PC acyl chains in a way that mimics solvation in neat liquids, we would expect the d^+ band to always carry intensity in a VSF spectrum due to torsional distortion along the carbon backbone. Results presented below provide clear evidence that the organic solvent interferes with acyl chain ordering in the monolayer, with the most dramatic effects observed for monolayers composed of longer chain phosphatidylcholine species (i.e., DPPC and DSPC).

In addition to the two symmetric stretch bands (d^+ and r^+), other vibrational transitions appear in the VSF spectra. These include the asymmetric stretches of the methylene (d^-) and methyl (r^-) groups, Fermi resonances from overtones of methylene and methyl bending modes, and the symmetric stretch of those methyl groups attached to the quaternary ammonium of the PC headgroup. Additional features arising from CH motion on the glycerol backbone appear only weakly in these spectra and are indistinguishable from the methylene Fermi resonance. Table 1 summarizes the relevant vibrational features, their frequencies, and the polarization conditions under which they appear.

IV. Results and Discussion

A. Molecular Orientation: Sampling Contributions to $\chi^{(2)}$. As indicated by eqs 3a–3c, different polarization choices for the incident and outgoing optical fields result in markedly different spectra of the same interface. The appearance and relative intensities of vibrational bands under the different polarization conditions elucidate molecular orientation of molecules adsorbed at the interface. Figure 3 shows three spectra of a tightly packed DLPC monolayer adsorbed to the water–CCl₄ interface, taken under different polarization conditions.

According to eq 3a the selection of p polarized sum frequency signal arising from p polarized visible and p polarized infrared (ppp) samples all nonzero elements of the $\chi^{(2)}$ tensor, $\chi_{zzz}^{(2)}$, $\chi_{izi}^{(2)}$ ($=\chi_{iiz}^{(2)}$), and $\chi_{iiz}^{(2)}$. Accordingly, all allowed vibrational transitions appear in a ppp spectrum (Figure 3, Table 1). These transitions include the symmetric stretch bands for the methylene (d^+) and methyl (r^+) groups at 2850 and 2874 cm⁻¹, respectively; a broad, featureless band from ~2890 to 2910 cm⁻¹ assigned to a methylene Fermi resonance interaction with CH₂ bending overtones; and a methyl asymmetric stretch (r^-) at 2960 cm⁻¹. Acyl stretches associated with the PC glycerol backbone and headgroup may also contribute to the weak signal at ~2900 cm⁻¹. The largest band in the spectrum appears at 2935 cm⁻¹. Various reports have assigned this feature to the methylene asymmetric stretch (d^-), a methyl Fermi resonance, or both.^{47,55} On the basis of previous deuteration studies of alkyl surfactants carried out in this laboratory,⁴³ we conclude that most of this

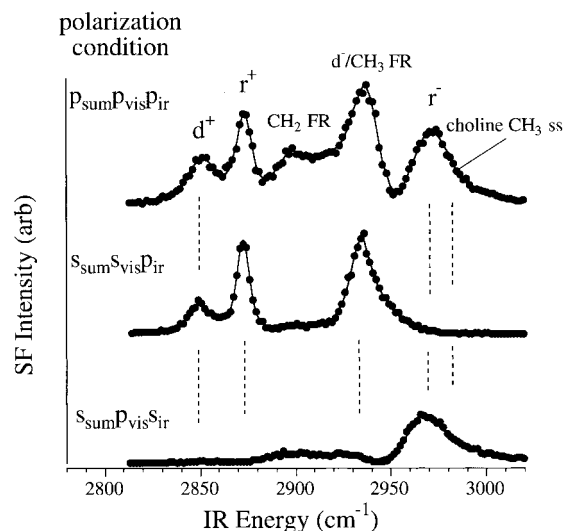


Figure 3. Spectra of a tightly packed DLPC monolayer (55 Å²/molecule) recorded under different polarization conditions. The top panel shows the spectrum recorded under ppp (sum, visible, ir) conditions. This choice of polarizations samples all four nonzero elements of the $\chi^{(2)}$ tensor. Vibrational band assignments are summarized in Table 1. The ssp spectrum (middle) samples CH stretching motion normal to the interface, while the sps spectrum (bottom) probes vibrational motion in the plane of the interface. Solid lines show fits to the data using a Voigt profile to account for natural (Lorentzian) line width of the transition, as well as the finite (Gaussian) bandwidth of the infrared source (6 cm⁻¹).

band's intensity arises from the methylene asymmetric stretch, although the methyl Fermi resonance may appear as a shoulder to the high-energy side. Also apparent at high surface concentrations is a high-energy shoulder on the r^- peak. Deuteration studies allow us to assign this feature, nominally at 2985 cm⁻¹, to the symmetric stretch of those methyl groups attached to the quaternary ammonium on the phosphatidylcholine headgroup. This assignment agrees with data from Raman studies of crystalline PC species.⁶¹

In an ssp spectrum (middle panel, Figure 3), only a single $\chi^{(2)}$ element, $\chi_{iiz}^{(2)}$, contributes to the observed spectral intensity. Consequently, an ssp spectrum is less congested than one taken under ppp conditions. The only features that appear are r^+ , d^+ , a weak signal from the methylene Fermi resonance, and the d^- /methyl Fermi resonance band. The two most striking differences between an ssp spectrum and a ppp spectrum are the disappearance of the r^- band in the ssp spectrum and an intensity reduction in the methylene Fermi resonance region. These changes reveal important information about acyl chain conformation within the monolayer. As discussed above, for a vibration to have a nonzero $\chi_{iiz}^{(2)}$ term, it must have its infrared transition dipole aligned normal to the interface. This symmetry constraint, coupled with the absence of r^- in the ssp spectrum, implies that on average the C₃ axes of the methyl groups lie normal to the interface. Low intensity in the 2890–2910 cm⁻¹ region suggests two things. First, any features in this region due to CH stretching on the headgroup or glycerol backbone do not contain a component of their infrared transition moment normal to the interface. Second, the methylene Fermi resonance is weak, meaning that d^+ (from which the methylene Fermi resonance derives intensity) carries very little oscillator strength. In fact, we can readily see in the spectrum that d^+ appears with considerably less relative intensity than r^+ . A weak d^+ band

(61) Bunow, M. R.; Levin, I. W. *Biochim. Biophys. Acta* **1977**, *489*, 191–206.

implies that the acyl chains have assumed primarily all-trans conformations (*vide supra*).

A spectrum taken under sps conditions is shown in the bottom panel of Figure 3. Dominating the spectrum is the r^- band at 2960 cm^{-1} . To the high-energy side of this feature lies the symmetric stretch of the choline methyl groups. Broad unresolved features from 2880 to 2940 cm^{-1} are difficult to assign definitively. In this region, one expects to find contributions from alkyl groups on the glycerol backbone as well as the choline headgroup and acyl chain methylene Fermi resonances. The d^+ band shows up very weakly at 2850 cm^{-1} , while r^+ is absent. According to eq 3c the sps polarization condition samples $\chi_{izi}^{(2)}$. For $\chi_{izi}^{(2)}$ to be nonzero, a vibration must have its infrared transition dipole aligned parallel to the interface. The behavior of the methyl vibrational features in the sps and ssp spectra is entirely self-consistent. In the sps spectrum, r^- appears with strong intensity while r^+ is absent. Conversely, in the ssp spectrum, r^+ is sharp and strong while r^- does not appear at all. Intensity information contained in the sps spectrum further strengthens the claim that the C_3 axes of the methyl groups lie, on average, normal to the interface.

B. Concentration Dependence of Monolayer Order. Monolayers of phosphatidylcholine monomers at the liquid–liquid interface form from the adsorption of monomers extracted from aqueous phase PC vesicles. The surface concentration of these monolayers depends on both the bulk aqueous PC concentration and the lipid bilayer phase of the PC vesicles.³⁷ When the vesicle bilayer is in its more fluid liquid crystalline form, vesicles readily deposit monomers at the interface and tightly packed monolayers form at bulk PC concentrations of $\sim 2\text{ }\mu\text{M}$.³⁷ Bulk concentrations below this limit lead to formation of more expanded monolayers. We monitor the extent of monolayer formation by recording the equilibrium surface pressures (π) for PC solutions of different concentrations in contact with a CCl_4 subphase. A representative isotherm for aqueous solutions of DLPC vesicles in contact with carbon tetrachloride at room temperature ($23\text{ }^\circ\text{C}$) is shown in Figure 4. With a gel–liquid crystalline phase transition temperature of $-1\text{ }^\circ\text{C}$, the lipid bilayers of DLPC vesicles at room temperature lie well above their melting point and the interfacial pressure rises steeply at sub-micromolar PC bulk concentrations. By bulk PC concentrations of $\sim 2\text{ }\mu\text{M}$, the isotherm has leveled out at an interfacial pressure of 42 mN/m . This limiting pressure agrees with literature values for PC monolayers in their liquid condensed/solid coexistence region at other organic–aqueous interfaces.^{19,23,45}

The inset of Figure 4 recasts the DLPC isotherm in terms of the Gibbs equation. Relating surface pressure to surface coverage and bulk PC concentration, the Gibbs equation allows one to calculate interfacial concentration of PC monolayers according to the expression⁶²

$$\Pi = 2nkT \ln(c) \quad (7)$$

where k is Boltzmann's constant, Π is the lateral surface pressure (mN/m), T is the temperature (K), c is the bulk PC concentration (mole fraction), and n corresponds to the number of adsorbed molecules per unit area. From this analysis we find that DLPC forms a tightly packed monolayer with a molecular area of $55 \pm 7\text{ }\text{\AA}^2/\text{molecule}$. This result lies reasonably close to values obtained for PC monolayers at alkane–water interfaces^{19,23} as well as at the air–water interface,⁴ suggesting that the limiting

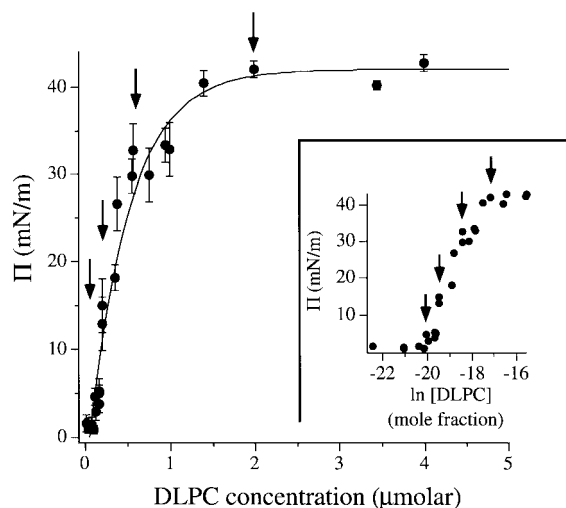


Figure 4. Representative isotherm depicting monolayer formation at the water– CCl_4 interface from an aqueous solution of phosphatidylcholine vesicles at a temperature above their gel–liquid crystalline transition temperature. These data describe the ambient temperature ($23\text{ }^\circ\text{C}$) behavior of DLPC solutions having various bulk concentrations. The solid line serves as a guide for the eye. The inset shows the same data with surface pressure plotted versus the natural log of bulk DLPC concentration in mole fraction. From these data we calculate that solutions of PC vesicles at temperatures above their transition temperatures and at concentrations greater than $\sim 2\text{ }\mu\text{M}$ form monolayers at the water– CCl_4 interface with surface coverages of $55\text{ }\text{\AA}^2/\text{molecule}$.

constraint on monolayer surface concentration is the solvated, zwitterionic choline headgroup. Simple geometric considerations support this picture: acyl chains have a cross-sectional area of $21\text{ }\text{\AA}^2$,⁶² and a hard sphere model of the choline headgroup fills $47\text{ }\text{\AA}^2$.^{4,26} Molecular modeling calculations indicate that the zwitterionic headgroup lies roughly parallel to the interface, meaning that the acyl chains are not as closely packed as their van der Waals radii would allow.²⁵ The difference between the calculated hard sphere headgroup area and our measured value may arise from the solvation sphere around the charged phosphate and choline functional groups.

At this juncture, we address an apparent discrepancy arising from analyzing the surface pressure data by means of the Gibbs equation. Typically, the Gibbs equation is applied to systems of adsorbed, soluble monolayers in reversible equilibrium with a bulk solution of surfactants.⁶² For phosphatidylcholines with chain lengths greater than C_{10} , monomers appear to adsorb irreversibly to the water– CCl_4 interface. Once a tightly packed monolayer has formed, the interfacial pressure becomes invariant to changes in temperature and bulk PC concentration,³⁷ meaning that the phosphatidylcholine monolayers in these studies technically should be treated as Langmuir monolayers. However, previous experiments have shown that monolayers formed from sparingly soluble lipids are equivalent regardless of whether they form from adsorption or from a spreading solvent.^{8,63} If we consider monolayer formation to represent a slow approach to equilibrium accompanied by a significant reduction in the free energy of the products (adsorbed monomers), then we would expect the monomers to be, in effect, irreversibly adsorbed. Enthalpic and entropic considerations suggest that a prohibitively large barrier frustrates monomer desorption back into the aqueous phase. Alkane chains experience rather large, exo-

(62) Davies, J. T.; Rideal, E. K. *Interfacial Phenomena*; Academic Press: New York, 1963.

(63) Nakagaki, M.; Funasaki, N. *Bull. Chem. Soc. Jpn.* **1974**, *47*, 2094–2098.

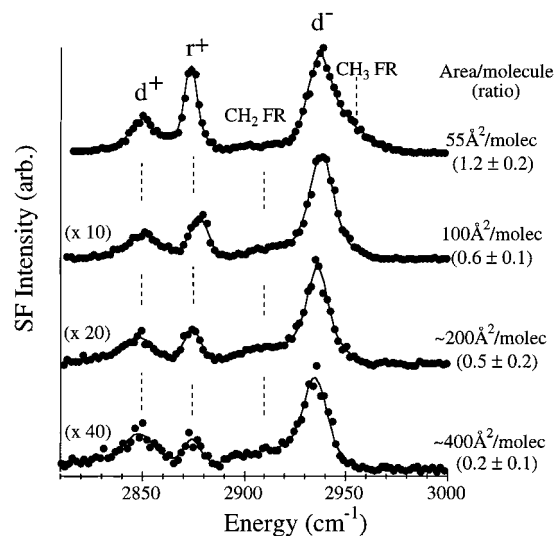


Figure 5. VSF spectra of DLPC monolayers having different surface coverages (points are marked on the DLPC isotherm in Figure 4). The r^+/d^+ ratios indicating the degree of molecular ordering are listed underneath the monolayer surface coverages. Spectra are multiplied by appropriate factors (in parentheses to the left of each spectrum) so that spectra may be viewed on the same scale. Spectral features were fit to Voight profiles. Relative intensities in going from spectrum to spectrum are accurate to within 25%. Error bars in the r^+/d^+ ratios reflect accuracy limits in spectral fitting routines as well as uncertainties in repeated measurements with numerous samples having the same surface concentration. Table 2 summarizes these results.

thermic heats of solvation in CCl_4 (~ 4.5 kJ/mol per CH_2 unit⁶⁴) so even the shortest chain phosphatidylcholine species in this work (DLPC) has an enthalpic barrier to monomer desorption of ~ 50 kJ/mol. In addition, monomer desorption would require considerable reordering of the water molecules around the acyl chains (hydrophobic effect), making the process entropically unfavorable as well. These two issues account for the observed irreversible adsorption of PC monomers as well as the lopsided partitioning of PC monomers into lamellar bilayers relative to the free, solvated monomer in the aqueous phase.⁶⁵

Using a Gibbs equation analysis allows us to calculate explicit surface coverages, which we would be unable to do otherwise. In previous studies, PC monolayers at various alkane–water interfaces were created by first spreading the PC monomers on top of the aqueous phase by means of a spreading solvent and then depositing the organic phase on top of the monolayer.^{18,21} This approach allowed exact determination of monolayer surface concentrations. In our experiments, the organic phase (CCl_4) rests below the aqueous phase and most spreading solvents are soluble in the CCl_4 . We have no well-defined way of depositing a specified PC concentration at the interface, which leads us to explore alternative methods of determining interfacial surface coverages. Agreement between terminal surface pressures and maximum surface concentrations from a Gibbs equation analysis and values reported from studies of spread monolayers at alkane–aqueous interfaces instills confidence in our approach.

The spectra of the DLPC monolayers formed at different bulk concentrations reflect the changes in molecular structure accompanying the changing surface concentration. Shown in Figure 5 are spectra of DLPC monolayers at different surface coverages corresponding to the arrows in the Figure 4 inset. Surface areas for each spectrum appear in the right-hand margin.

(64) Fuchs, R.; Chambers, E. J.; Stephenson, W. K. *Can. J. Chem.* **1987**, *65*, 2624–2629.

(65) Nichols, J. W. *Biochemistry* **1985**, *24*, 6390–6398.

Table 2. DLPC Integrated Intensity Ratios vs Surface Concentration and Temperature

surface concentration (Å ² /molecule)	r ⁺ /d ⁺ ratio	temp (°C)	r ⁺ /d ⁺ ratio
400	0.2 ± 0.1	9	1.7 ± 0.2
200	0.5 ± 0.2	15	1.7 ± 0.3
100	0.6 ± 0.1	19	1.8 ± 0.2
55	1.2 ± 0.2	23	1.2 ± 0.1(5)
		25	1.1 ± 0.2
		29	1.1 ± 0.2(5)
		35	0.9 ± 0.2

Spectra were recorded under the ssp conditions and multiplied by an appropriate factor to place all spectra on the same scale. Although the same features appear in the different spectra, relative intensities of vibrational bands change, indicating evolution in chain conformation as surface coverage increases. As mentioned in the acyl spectroscopy section, the integrated intensity of r^+ (methyl symmetric stretch, 2874 cm^{-1}) relative to d^+ (methylene symmetric stretch, 2850 cm^{-1}) provides a measure of conformational order among the acyl chains. When chains exist in an all-trans conformation, d^+ becomes symmetry forbidden and the r^+/d^+ ratio is large. Conversely, a small r^+/d^+ ratio suggests a high degree of conformational disorder within the acyl chains.

Figure 5 and Table 2 show that increasing surface coverage is accompanied by a corresponding increase in the r^+/d^+ ratio. The absolute intensities of all bands grow with increasing surface coverage, but r^+ grows preferentially, relative to d^+ . This trend is consistent with our ideas of the monolayer passing from an expanded, disordered arrangement to a tightly packed, well-ordered, two-dimensional solidlike structure at high surface concentrations. At all concentrations, d^+ is broader than r^+ , possibly reflecting the larger variation in methylene environments relative to methyl environments. The nominal methylene Fermi resonance band becomes vanishingly small at the highest surface coverages, consistent with the picture of acyl chains adopting more ordered conformations as the surface concentration increases. We note that at the highest surface concentrations the d^- band broadens asymmetrically to higher energy, a phenomenon we attribute to the growing contribution from the methyl Fermi resonance.

C. Temperature Dependence of Acyl Structure. Dynamic surface tension studies show that the temperature of a system affects the rate at which phospholipid monolayers form,⁶⁶ but the effect of temperature on the resulting monolayer structure has, thus far, remained unclear. Neutron diffraction studies of monolayers composed of single-chain, neutral surfactants adsorbed to an air–water interface indicate that a structural roughening of the monolayer occurs as the temperature increases.^{67,68} Furthermore, experiments carried out on ternary oil–water–surfactant emulsions show that increased temperatures induce deeper solvent penetration into both sides of the monolayer structure.⁶⁹

To address the relationship between temperature and monolayer structure, we formed tightly packed monolayers of DLPC

(66) Walker, R. A.; Richmond, G. L., submitted for publication.

(67) Penfold, J.; Staples, E.; Thompson, L.; Tucker, I.; Thomas, R. K.; Lu, J. R. *Ber. Bunsen-Ges. Phys. Chem.* **1996**, *100*, 218–223.

(68) Lu, J. R.; Li, Z. X.; Thomas, R. K.; Staples, E. J.; Thompson, L.; Tucker, I.; Penfold, J. *J. Phys. Chem.* **1994**, *98*, 6559–6567.

(69) Cavallaro, G.; Manna, G. L.; Liveri, V. T.; Aliotta, F.; Fontanella, M. E. *J. Colloid Interface Sci.* **1995**, *176*, 281–285.

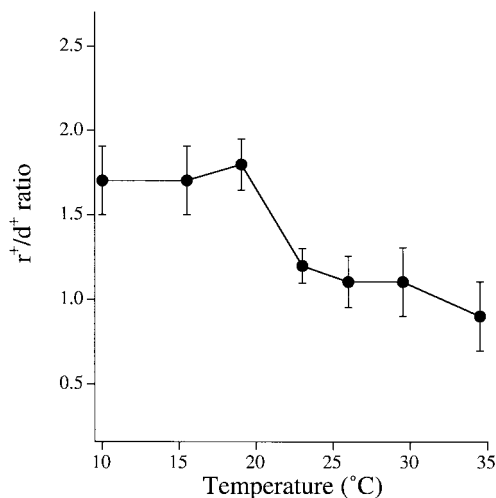


Figure 6. A plot of the r^+/d^+ ratios for a tightly packed DLPC monolayer at the water- CCl_4 interface as a function of temperature. Error bars represent standard deviations in multiple measurements with different samples. Table 2 summarizes these results.

adsorbed to the water- CCl_4 interface and then recorded spectra of the monolayer at different temperatures. Temperatures inside the cell were controlled by a circulating bath in channels passing through the aqueous phase. Temperatures were measured in both phases with a thermometer, and reported accuracies are ± 1 °C. We recorded spectra over a temperature range of 9–35 °C. The interface began to boil at temperatures higher than ~ 40 °C when both lasers (ω_{vis} and ω_{IR}) were present. In the absence of laser light, boiling of the interface occurred at temperatures above 55 °C. Carbon tetrachloride boils at 76 °C, but an aqueous overlayer effectively raised the vapor pressure of CCl_4 at the interface and reduces the solvent's boiling point. Over the temperature range sampled, lateral surface pressure remained constant at 42 mN/m, indicating that neither adsorption nor desorption accompanied changes in the system's temperature and the monolayer remained tightly packed.

Acyl chain structure in the DLPC monolayer shows a pronounced dependence on temperature. The ratio of r^+/d^+ remains constant at ~ 1.7 up to 19 °C. However, by ambient temperatures (23 °C) the ratio drops steeply to the 1.2 value reported in the previous section and decreases slowly with further increases in temperature. Figure 6 and Table 2 summarize these results. We do not interpret the change in r^+/d^+ occurring between 19 and 23 °C as a phase transition between distinct, two-dimensional, thermodynamic states. A phase transition would necessarily require a change in surface concentration and should show a temperature dependence on acyl chain length.^{19,21} However, surface tension measurements indicate that the surface concentration remains unchanged. Furthermore, preliminary measurements on alternative PC monolayers exhibit the same structure vs temperature dependence regardless of chain length (data not shown). We speculate that the r^+/d^+ behavior simply reflects more pronounced, thermally induced penetration of the CCl_4 solvent into the acyl chain layer. Over the temperature range investigated, the widths of the vibrational bands remain constant to within experimental uncertainty, indicating that the chains do not undergo radical changes in conformation. However, if chains occupy only 42 Å² (21 Å²/chain) of each monomer's 55 Å² area, there may very well exist unfilled volume in the acyl portion of the monolayer into which CCl_4 molecules can penetrate. As the chains become more thermally agitated, larger "voids" can open up and the monolayer becomes more permeable to solvent

Table 3. Monolayer Order vs Chainlength at Water- CCl_4 and Air-Water Interfaces

molecule	<i>n</i>	<i>T_c</i> (°C)	r^+/d^+ ratio		<i>r⁺/d⁺</i> ratio		fwhm (cm ⁻¹)		
			CCl_4 -water	air-water	<i>r⁺</i>	<i>d⁺</i>	<i>r⁺</i>	<i>d⁺</i>	
DLPC	12	-1	1.2 ± 0.1(5)		8	16	1.9 ± 0.5	22	25
DMPC	14	23	0.7 ± 0.2		9	16	2.1 ± 0.8	20	30
DPPC	16	41	0.5 ± 0.2		10	20	5.3 ± 1.1	23	30
DSPC	18	54	0.5 ± 0.2		10	18	11.9 ± 2.0	23	30

penetration. This picture is consistent with the predictions of molecular dynamics simulations on PC bilayers³⁵ as well as with results from ternary oil-water-surfactant emulsion systems. In addition, recent results from surface pressure measurements of DPPC and DSPC monolayers adsorbed at a water-dichloroethane (DCE) interface provide evidence that the DCE solvent is highly mobile in the monolayer surface phase.⁷⁰

D. Monolayer Order vs Chain Length (Liquid-Liquid).

To compare the degree of acyl chain order in monolayers composed of phosphatidylcholines having different chain lengths, we prepared tightly packed monolayers of four saturated, symmetric phosphatidylcholines with chain lengths of C₁₂ (DLPC), C₁₄ (DMPC), C₁₆ (DPPC), and C₁₈ (DSPC). At room temperature, aqueous solutions of DLPC and DMPC form tightly packed monolayers at bulk concentrations above 2 μM. Under similar conditions, both DPPC and DSPC form expanded monolayers with greatly reduced surface coverages. In earlier work, we attributed this behavior to differences in the thermodynamic phase of the various phosphatidylcholine vesicle bilayers.³⁷ At room temperature, DLPC vesicle bilayers (*T_c* = -1 °C) are in their fluidlike, liquid crystalline state, and DMPC vesicle bilayers (*T_c* = 23 °C) exist in a gel-liquid crystalline coexistence state. With transition temperatures of 41 and 54 °C, respectively, DPPC and DSPC vesicle bilayers remain frozen in their solidlike, gel state. Strong interchain attractions within the rigid bilayer inhibit adsorption of DPPC and DSPC monomers at the interface.

To induce formation of tightly packed DPPC and DSPC monolayers (55 Å²/molecule), we raised the temperature of the two liquid phases above the respective gel-liquid crystalline transition temperatures (Table 3) and monitored interfacial pressure. The interfacial pressure of these systems reached a maximum value of 42 mN/m and then leveled out, indicating formation of a tightly packed monolayer. Surface pressures in the 41–43 mN/m range are characteristic of PC monolayers in a compact liquid condensed/solid phase.^{18,19,45} Monolayer formation was also irreversible, as evidenced by a constant interfacial pressure as the system cooled to ambient conditions. In light of enthalpic and entropic considerations discussed earlier, this irreversible adsorption is not surprising.

After preparing tightly packed monolayers of the PC monomers, we examined how order among the acyl chains depends on chain length. Shown in Figure 7 are ssp spectra resulting from tightly packed monolayers composed of the different chain length phosphatidylcholines. Despite sharing similar surface concentrations, the monolayers of the different species show distinct differences in their degree of ordering. Comparing the integrated intensity of r^+ relative to d^+ indicates that the monolayer composed of the shorter chain DLPC species contains less acyl chain disorder than monolayers made up of the longer chain phosphatidylcholines. Table 3 summarizes the r^+/d^+ ratio data. The DLPC monolayer exhibits a relatively large r^+/d^+ ratio of 1.2 (± 0.2). All other monolayers, however, have smaller r^+/d^+ ratios (~ 0.6) which are almost equivalent to within

(70) Grandell, D.; Murtomäki, L. *Langmuir* **1998**, *14*, 556–559.

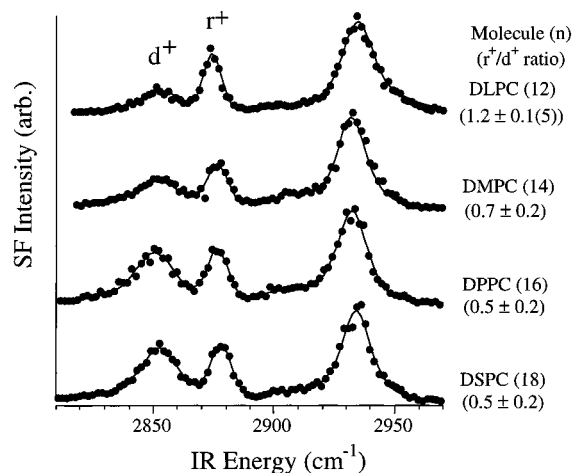


Figure 7. VSF spectra of tightly packed monolayers composed of DLPC ($n = 12$), DMPC ($n = 14$), DPPC ($n = 16$), and DSPC ($n = 18$) at the water- CCl_4 interface. Ratios of r^+/d^+ appear underneath the PC acronyms. Spectral features were fit to Voigt profiles. Relative intensities in going from spectrum to spectrum are accurate to within 15%. Error limits in the r^+/d^+ ratios reflect the accuracy of spectral fitting routines as well as uncertainties in repeated measurements both on the same sample and different samples having the same surface concentration. Table 3 summarizes these results.

experimental uncertainty, although the DMPC monolayer does appear to be slightly more ordered than the DPPC and DSPC monolayers. These effects presumably arise due to differences in acyl chain length rather than laterally induced disorder, given that all four species share the same surface coverage.

In all four spectra, the integrated r^+ intensity remains roughly the same. Differences between the DLPC and the remaining three spectra arise from changes in the integrated intensity of the d^+ band. This observation suggests that for phosphatidylcholines having chains lengths greater than C_{12} increasing chain length does not affect the degree of chain-chain interaction within the monolayer. We hypothesize that the CCl_4 solvent intercalates between the acyl chains of the phosphatidylcholine monolayers and effectively screens the chains from each other, minimizing any intermolecular van der Waals attractions that would otherwise serve to increase order with increasing chain length. On the basis of the geometrical considerations described above, CCl_4 solvent molecules should be small enough to slip into the acyl chain network.

Interestingly, different methods of monolayer preparation can affect the degree of order found among the acyl chains. The monolayers described above were formed from the decomposition of PC vesicles in their liquid crystalline state, and the interface itself remained undisturbed during the process. Recently, a new preparation procedure demonstrated that highly ordered monolayers of longer chain PCs can be formed at the water- CCl_4 interface by means of multiple injections of a PC bilayer solution into the aqueous phase.³⁸ Successive injections physically perturb the interface, and the resulting DSPC monolayer has an r^+/d^+ ratio of ~ 4.5 . Apparently, these later additions force a compression of the existing monolayer, which expels any solvating CCl_4 in the acyl chain network. Expulsion of the organic solvent results in a two-dimensional crystallization of the monolayer. Due to stronger attractive forces between C_{18} chains, crystallized monolayers of DSPC show a higher degree of order than monolayers composed of shorter chain species, similar to observations for phosphatidylcholine monolayers at the air-water interface.

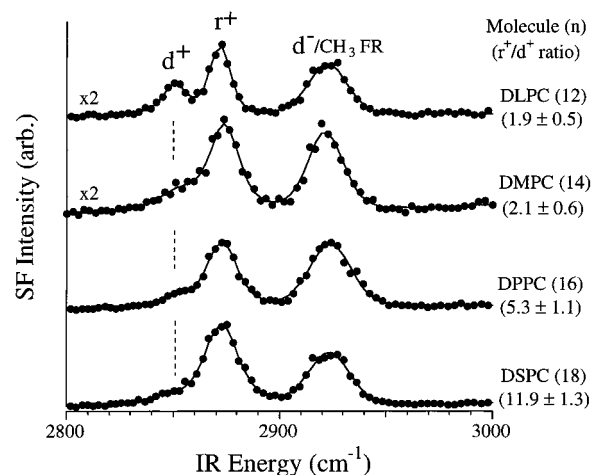


Figure 8. VSF spectra of tightly packed monolayers composed of DLPC ($n = 12$), DMPC ($n = 14$), DPPC ($n = 16$), and DSPC ($n = 18$) at the air-water interface. Ratios of r^+/d^+ appear underneath the PC acronyms. Spectral features were fit to Voigt profiles, although the solid lines in the spectra serve only as guides for the eye. Relative intensities in going from spectrum to spectrum are accurate to within 15%. Error limits in the r^+/d^+ ratios reflect the accuracy of spectral fitting routines as well as uncertainties in repeated measurements both on the same sample and different samples having the same surface concentration. Table 3 summarizes these results.

E. Monolayer Order vs Chain Length (Air-Water). To compare the acyl chain structure of phosphatidylcholine monolayers formed by vesicle decomposition at the CCl_4 -water interface with those at the air-water interface, we prepared monolayers at the air-water interface from solutions of phosphatidylcholines dissolved in a spreading solvent (hexane-ethanol, 4:1). Formation of tightly packed monolayers at the air-water interface typically required deposition of $\sim 50 \mu\text{L}$ of the spreading solvent dispersed in uniform drops on the water surface. PC surface concentrations were calculated to be $55 \pm 4 \text{ \AA}^2/\text{molecule}$, and all four monolayers exhibited surface pressures of 45 mN/m in excellent agreement with literature values.⁴

Shown in Figure 8 are the ssp spectra of the four different phosphatidylcholine monolayers adsorbed to the air-water interface. Spectra for DLPC and DMPC have been multiplied by a factor of 2 in order to put them on the same scale as the DPPC and DSPC spectra. Spectral stability in both relative and absolute intensities over the span of 3 days indicated that the volatile spreading solvent did not remain trapped in the monolayer and influence acyl chain structure. These spectra were recorded using the Ti:sapphire picosecond laser system described in the Experimental section. Although the infrared beam had a frequency bandwidth of only 16 cm^{-1} , compared to 6 cm^{-1} for the nanosecond system, both r^+ and d^+ remain distinguishable in the spectra even as d^+ becomes nothing more than a weak, low-energy shoulder on the r^+ band in the DPPC and DSPC spectra. Furthermore, the increased bandwidth does not artificially influence the r^+/d^+ ratio. Spectra of PC monolayers at the aqueous- CCl_4 interface acquired with the picosecond system exhibited r^+/d^+ ratios identical to those acquired with the nanosecond system.

Two trends are apparent in Figure 8. First, r^+ signal levels for the two longer chain phosphatidylcholines are appreciably larger than those for the two shorter chain species. Given that all four monolayers share the same surface concentration (hence the same number of contributing methyl groups), this trend suggests that methyl groups of longer chain species have a larger

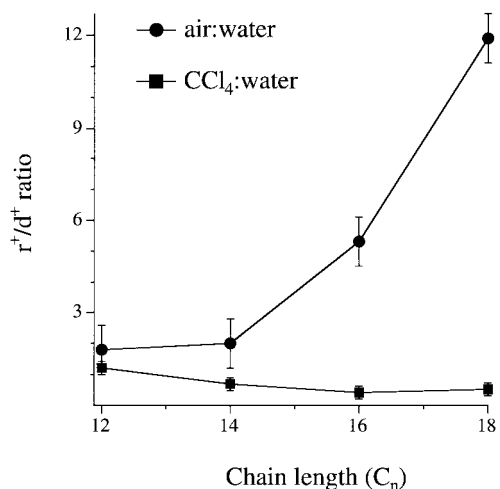


Figure 9. A comparison of the r^+/d^+ ratios for the different PC monolayers at the air–water and water– CCl_4 interfaces. Error bars reflect the uncertainty limits already discussed.

component of their infrared transition dipole aligned normal to the interface. Monolayers composed of the four phosphatidylcholines do not exhibit any long-range orientational order, as evidenced by an absence of r^- in all four spectra. Second, the degree of order among the acyl chains appears to increase dramatically with increasing chain length. Monolayers of DLPC and DMPC evince a similar degree of acyl order ($r^+/d^+ \sim 2$), although the d^+ band of the DMPC monolayer has broadened considerably. Monolayer characteristics change, however, when the DMPC and DPPC spectra are compared. The absolute integrated intensity of the DPPC d^+ band drops by $\sim 25\%$ compared to the same feature in the DMPC spectrum. At the same time the intensity of the DPPC r^+ band is almost twice that of r^+ in the DMPC spectrum, leading to a DPPC r^+/d^+ ratio in excess of 5. This trend continues in the DSPC spectrum where d^+ loses $\sim 50\%$ of the intensity it has in the DPPC monolayer. The r^+ band carries approximately the same intensity in the DSPC monolayer as it does in the DPPC monolayer, and the DSPC r^+/d^+ ratio approaches 12 (Table 3). This behavior implies that acyl chains in tightly packed monolayers at the air–water interface assume more of an all-trans conformation as chain length increases. Without an organic solvent to screen the chains from each other, attractive interchain forces grow with increasing chain length, leading to greater conformational order in monolayers formed from longer chain phosphatidylcholine species.

F. Monolayer Order Comparison (Liquid–Liquid vs Air–Water). Figure 9 highlights the disparity in acyl chain structure between PC monolayers adsorbed to the water– CCl_4 interface and PC monolayers adsorbed to the air–water interface. The comparison illustrates several important points. Although disorder in the water– CCl_4 monolayer increases with increasing PC chain length, the overall effect is minimal when compared to the dependence of monolayer order on chain length at the air–water interface. Data from DPPC and DSPC monolayers in the two different environments provide the clearest evidence that at the liquid–liquid interface the organic carbon tetrachloride solvent effectively screens the acyl chains from each other. Drawing this conclusion on the basis of the DLPC and, to a lesser extent, the DMPC data is more tenuous. In fact, taking into account the uncertainty associated with the DLPC measurements at the CCl_4 –water and air–water interfaces (1.2 ± 0.2 liquid–liquid vs 1.9 ± 0.5 air–water), the degree of conformational order found within the monolayer is

rather similar. For the shorter chain PC species at the liquid–liquid interface, the organic carbon tetrachloride solvent apparently does not solvate the acyl chains nearly so well as it does those of the longer chain phosphatidylcholines.

At first glance this observation that DLPC monolayers exhibit a similar degree of order at the two different interfaces seems to disagree with the recent molecular dynamics simulations of simple, charged surfactant monolayers at the air–water and water–carbon tetrachloride interfaces.⁷¹ Schweighofer et al. found that dodecyl sulfate molecules, anionic surfactants with a single C_{12} chain, adsorbed to the air–water interface exhibited a pronounced preference to bend close to the solvated sulfate group and incorporate a gauche defect into the alkyl chain. This geometry allows the dodecyl sulfate chains to lie flat on the water surface and maximizes their van der Waals contact. When adsorbed to the water–carbon tetrachloride interface, the dodecyl sulfate chains contain much less distortion and extend into the organic phase at an angle of approximately 40° from the interfacial normal.⁷¹

Before attempting to compare the results of these simulations with the experiments carried out on the tightly packed DLPC monolayers, two important points should be considered. First, the simulations were carried out at very low surfactant surface concentrations ($\sim 600 \text{ \AA}^2/\text{molecule}$),⁷¹ while the experimental DLPC surface concentration was considerably higher ($55 \text{ \AA}^2/\text{molecule}$). Taking into account that each adsorbed DLPC monomer contains two C_{12} chains makes the monolayer chain density even higher ($\sim 28 \text{ \AA}^2/\text{chain}$). Simulations carried out on high surface coverage monolayers at the air–water interface have found that chain–chain interactions between adsorbed monomers leads to a straightening of the chains as they pull away from the water surface.⁷² Including more surfactants in simulations of the water– CCl_4 interface would probably have only minimal effect on chain orientation, given that the alkyl chains already stand away from the interface. In fact, more recent work has examined water–carbon tetrachloride interfaces with higher surfactant surface coverages ($45 \text{ \AA}^2/\text{molecule}$), but these studies only address issues pertaining to water structure and dynamics in the interfacial region, not the structure and orientation of the alkyl chains.⁷³

Second, a closer inspection of the simulation results shows that apart from chain geometry at the C_{11} – C_{12} position (the first C–C bond after the sulfate group), dodecyl sulfate surfactants at the air–water and water–carbon tetrachloride interfaces share remarkably similar geometries. Schweighofer et al. present statistics for the 11 dihedral angles found in a dodecyl sulfate molecule.⁷¹ With only three notable exceptions, the fraction of gauche defects in the various dihedral angles of molecules adsorbed at the two different interfaces are equivalent to within 10%. In other words, dodecyl sulfate molecules at the air–water and water–carbon tetrachloride interfaces show the same propensity for trans/gauche conformations in 8 of the 11 dihedral angles. The major differences in chain conformation occur in three of the five dihedral angles closest to the sulfate headgroup. Incorporating defects into this part of the molecule allows the dodecyl chain to bend over at the air–water interface so as to maximize its contact with the water surface. With C_{12} alkyl chains packed much more closely together, as in the air–water experiments described above, the hydrocarbon tails should

(71) Schweighofer, K. J.; Essmann, U.; Berkowitz, M. *J. Phys. Chem. B* **1997**, *101*, 3793–3799.

(72) Böcker, J.; Schlenkrich, M.; Bopp, P.; Brickmann, J. *J. Phys. Chem.* **1992**, *96*, 9915–9922.

(73) Schweighofer, K. J.; Essman, U.; Berkowitz, M. *J. Phys. Chem. B* **1997**, *101*, 10775–10780.

not experience a strong driving force to lie down at the interface. Rather, chains should stand upright. The molecular dynamics simulations indicate that outside of the first few dihedral angles nearest the headgroup the C_{12} chains ought to enjoy conformations similar to those of chains at the water- CCl_4 interface, which would agree with the experimental measurements of DLPC monolayer order at the two interfaces. An interesting test of this idea would involve simulating higher surface concentrations of longer chain species at both the air-water and water- CCl_4 interfaces where experimental data indicate that noncovalent interchain interactions play a much stronger role in determining order within the monolayer (Figure 9).

A number of different studies have suggested that the nature of an organic solvent can dramatically affect the degree of order found within phospholipid monolayers.^{14,23,36} When the chain length of the organic solvent matches the length of the phospholipid alkyl tails, fluorescence microscopy experiments indicate that the solvent intercalates into the alkyl chain network and the monolayer becomes considerably more ordered upon compression.²³ In contrast, organic solvents with chain length mismatch or saturated rings do not form a well ordered, homogeneous, mixed condensed phase and are excluded from the phospholipid alkyl chain network at all stages of compression. Differential scanning calorimetry and X-ray diffraction experiments on bilayers support these findings. On the basis of the effects of chain length matched and unmatched solvents on bilayer transition temperatures and structure, McIntosh et al. postulated that chain length matched solvents line up among the phospholipid alkyl chains, while unmatched solvents congregate in the center volume of the bilayer interior.³⁶ Interestingly, these same studies on bilayers found that small molecules (methanol and chloroform) reduced and broadened the bilayer gel-liquid crystalline transition temperature, indicating that the small volume solvents permeated into the monolayer alkyl chain network and at least partially solvated the chains. In the experiments described above we believe that the small, spherical CCl_4 solvent molecules behave like their more polar counterparts, solvating the alkyl chains in the monolayer. On the basis of these studies^{14,23,36} we conclude that we should be able to study highly ordered phosphatidylcholine monolayers adsorbed to liquid-liquid interfaces, provided that sufficiently pure, optically transparent (from 3.2 to 3.6 μm), deuterated long-chain organic solvents can be procured.

V. Conclusions

Experiments described in this work demonstrate how vibrational sum frequency spectroscopy used in conjunction with traditional surface science techniques can provide very detailed information about phosphatidylcholine monolayers adsorbed to a liquid-liquid interface. By measuring the surface activity of aqueous solutions containing phosphatidylcholine vesicles, we map out isotherms for monolayer formation which can then be manipulated to calculate monolayer surface coverages. Vibrational spectra of these adsorbed monolayers contain data which explicitly show how conformational order within the monolayer depends on different experimentally controlled variables.

Taking advantage of the symmetry constraints imposed upon the nonlinear susceptibility tensor (χ^2) at the interface, we observe how different choices of incident and outgoing polarizations leads to markedly different spectra of the same DLPC monolayer adsorbed to the water- CCl_4 interface. The appearance of different vibrational bands, specifically the methyl symmetric and asymmetric stretches, under different polarization conditions provides strong evidence that tightly packed mono-

layers at the liquid-liquid interface do not exhibit long-range orientational tilt, in contrast to monolayers adsorbed to more rigid, solid substrates. On average the C_3 symmetry axes of the acyl methyl groups at the liquid-liquid interface align perpendicular to the interface instead of having a well-defined, preferred tilt angle such as that found for self-assembled monolayers at air-solid interfaces.⁷⁴

Conformational order within the monolayer is determined by comparing the integrated intensity of the methyl symmetric stretch (r^+) to the integrated intensity of the methylene symmetric stretch (d^+). As a DLPC monolayer becomes increasingly concentrated, it also becomes increasingly well-ordered. These results appeal to intuition because they imply that as the monolayer surface coverage increases the acyl chains of the adsorbed DLPC monomers have less volume to sweep out. The chains proceed to stand up and assume more of an all-trans conformation as evidenced by the largest r^+/d^+ ratios at the highest surface concentrations. This effect is much less pronounced for the longer chain phosphatidylcholine species,³⁷ suggesting that increased chain length leads to a higher permeability of the monolayer to the organic CCl_4 solvent.

The temperature dependence of order within DLPC monolayers implies the existence of a barrier to monolayer permeability. At temperatures below 19 °C, order within a tightly packed DLPC monolayer seems invariant, as evidenced by a steady r^+/d^+ ratio of 1.7. Above 19 °C, however, the r^+/d^+ ratio diminishes, implying the onset of thermally induced disorder among the acyl chains. Surface pressure measurements indicate that the surface concentration does not change and the observed effect does not result from a two-dimensional phase transition. These data, along with molecular dynamics simulations³⁵ and results from neutron⁶⁷ and ternary oil-water-surfactant emulsion experiments,⁶⁹ strongly suggest that the increased disorder arises from solvent penetration into the hydrocarbon chain network. At higher temperatures, the acyl chains become more thermally agitated, effectively making the monolayer more "spongy" and susceptible to CCl_4 permeation.

The degree of ordering within tightly packed phosphatidylcholine monolayers adsorbed to the water- CCl_4 interface depends on acyl chain length. At equivalent surface concentrations, shorter chain species form monolayers more ordered than those of longer chain species, as demonstrated by their respective r^+/d^+ ratios. In contrast, at the air-water interface, monolayers of the longer chain species are much more ordered than monolayers of the shorter chain species. We interpret this difference as evidence that under ambient conditions the CCl_4 solvates the alkyl chains of monolayers adsorbed to the water- CCl_4 interface. Monolayers composed of longer chain species (i.e., DPPC and DSPC) are more easily solvated than monolayers of shorter chain species (i.e., DLPC and DMPC), and the reduction in interchain attractive forces leads to greater propensity for torsional distortion and gauche defects. At the air-water interface, the acyl chains in the monolayer are not screened from each other. Longer chains experience stronger interchain van der Waals forces and form monolayers correspondingly more ordered than those of their shorter chain counterparts.

Experiments described in this work provide molecular level insight into how phosphatidylcholine monolayers order at a liquid-liquid interface and how the degree of ordering depends on variables such as surface concentration, temperature, and the presence of a spherical, nonpolar organic solvent (CCl_4).

(74) Porter, M. D.; Bright, T. B.; Allara, D. L.; Chidsey, C. E. D. *J. Am. Chem. Soc.* **1987**, *109*, 3559-3568.

Previously, such systems could only be characterized by thermodynamic techniques or by methods which incorporated fluorescent probes and were sensitive to structural details on the micrometer level. By means of vibrational sum frequency spectroscopy, a second-order nonlinear optical technique with inherent surface specificity, we can now examine the vibrational structure of adsorbed phosphatidylcholine monomers and infer details about molecular orientation and structure. This work only scratches the surface of the types of experiments which can be performed with these systems. The temperature-dependent studies carried out on DLPC monolayers suggest an extensive list of experiments designed to test ideas about thermally induced solvent permeation of the monolayer acyl chain network. Selectively deuterating phosphatidylcholine species should lead to a more detailed picture of how various

parts of the adsorbed molecules orient themselves at the interface. To extend the findings presented above to more biologically pertinent systems, phospholipid monolayers of mixed composition can be studied.

Acknowledgment. The authors thank Dr. Beth Smiley for helpful discussions and for carrying out dynamic light scattering experiments to determine vesicle size in aqueous phosphatidylcholine solutions. The authors also thank Dr. Dick Brennan and the Oregon Health Sciences University for use of the dynamic light scattering equipment. J.A.G. acknowledges support through the NSF-REU program (CHE-9531402). Funding from the National Science Foundation (CHE-9725751) and the Office of Naval Research is gratefully acknowledged.

JA980736K